EUROPEAN COMMISSION

RESEARCH DG

MARIE CURIE MOBILITY ACTIONS

REINTEGRATION ACTIONS
PERIODIC SCIENTIFIC/MANAGEMENT REPORT

Project no. 517581
Project acronym XFLOOD
Project full name

Advancing Quantitative Precipitation Estimation and Short-to-Medium Range Forecasting on the Basis of Remotely Sensed Data Assimilation

International Reintegration Grants (IRG)

Deliverable No 2

Methodology for retrieving precipitation from satellite observations

by

Emmanouil Anagnostou and Anastasios Papadopoulos

Period Number : 1

Due date of deliverable: 15/04/2006

Period covered: from 15/04/2005 to 14/04/2006

Date of preparation: 15/05/2006

Date of submission: 25/05/2006

Start date of project: 15/04/2005

Duration: 24 months

Project coordinator name: Dr. Evangelos Papathanassiou
Project coordinator organisation name: Hellenic Centre for Marine Research

Organisation name of lead contractor for this deliverable: Hellenic Centre for Marine Research

Project co-funded by the European Commission within the Sixth Framework Programme (2002-2006)
Dissemination in level PU (Public)

1. INTRODUCTION

Long-term precipitation observations at global scale are available mainly from passive microwave (PM) sensors onboard a number of earth orbiting satellites (TRMM, DMSP, EOS, NOAA), as well as visible and infrared (VIS/IR) sensors onboard geo-stationary platforms. The TRMM (Tropical Rainfall Measuring Mission) satellite is the first orbiter to carry a combination of active (Precipitation Radar, PR) and multi-channel passive microwave (TMI) sensors. These sensors advance our ability to estimate rainfall over both land and ocean (e.g., Grecu et al. 2004; Smith et al., 1997; Haddad et al., 1996). Rain retrieval from PR (or combination of PR and TMI over ocean) is associated with an unprecedented accuracy and resolution, but is limited in terms of sampling due to the narrow PR swath width (215 km). The TMI and PM sensors onboard other satellites provide wider coverage (760-1000 km), but their observations are associated with a more complex relationship to precipitation compared to the PR; particularly for overland retrieval. Additionally, PM observations offer only intermittent coverage of a given region of interest (currently this is approximately six to eight observations per day accounting for all available satellite platforms). Contrary, VIS/IR sensors offer more continuous global precipitation observations at the cost of being weakly associated to precipitation, which requires empirical relationships strongly dependant on calibration.

The Global Precipitation Climatology Project (GPCP—Adler et al. 2003) has advanced to the point of providing a multi-year (23+ years) 2.5-deg/monthly global precipitation climatology on the basis of precipitation estimates from different satellite sensors and gauge measurements. The satellite observations used in GPCP are the low-orbit PM data from the Special Sensor Microwave/Imager (SSM/I) that go back to the mid-1987, and the Infrared data from geo-stationary platforms that go back to 1979. The GPCP analysis used combination of algorithms for estimation of precipitation climatology from SSM/I. Satellite Infrared data were used in the pre-microwave era (before 1987) to extend satellite observations back to 1979. The Infrared precipitation algorithm was calibrated to the PM analysis of the later years to get consistency in the precipitation climatology. The merged satellite rainfall products were adjusted based on comparisons with gauges to remove systematic errors. However, there is room for improvement in certain aspects of the GPCP precipitation climatology that includes the derived PM rainfall fields and their aggregation to derive monthly datasets.

Monthly rainfall estimates from passive microwave observations have biases and random errors, which are due to three main sources: (1) uncertainties in the PM rain retrieval algorithms (Kummerow 1998), (2) the diurnal cycle of rainfall (Anagnostou et al. 1999), and (3) satellite sampling frequency (Bell et al. 1990). In the present work we have improved the accuracy of the GPCP global (land and ocean) precipitation climatology derived from SSM/I observations by addressing those issues.

The first issue was addressed by deriving improved SSM/I rain retrievals on the basis of TRMM data. For this purpose, we combined two newly developed rain estimation algorithms: (1) the Dinku and Anagnostou (2005a,b) (hereafter named DA05) for overland rainfall estimation, and the Bayesian SSM/I retrieval of Grecu and Olson (2005) (hereafter named GO05) for rainfall estimation over water surface. The GO05 algorithm is based on a global database of more definitive ocean precipitation profiles (and corresponding simulated passive microwave observations) derived from the Grecu et al. (2004) combined PR/TMI profiling algorithm. The basics of the two techniques and justification of their added value to current SSM/I precipitation estimates are discussed in the methodology.

The issue of diurnal rainfall variability effect was addressed using multi-year TMI rainfall estimates. The hypothesis was that eight years of TMI rainfall data would be an adequate sample to determine the mean diurnal cycle (MDC) of precipitation at 5-deg resolution over the Tropics and Sub-Tropics. MDC information then was used to derive adjustments to the fixed SSM/I overpass times over each 5-deg grid to represent mean daily rainfall conditions. The approach is described in the methodology section.

The third issue, namely, the overall satellite sampling effect that includes also residual effects from MDC corrections, was addressed by quantifying non-linear adjustments to the gridded (and MDC corrected) monthly SSM/I rainfall estimates. The adjustments were evaluated on the basis of the Anagnostou et al. (1999) statistical technique that utilizes common satellite-rain gauge monthly rainfall datasets. The technique uses an exponential function (whose argument is a polynomial of the rain variable) that represents the distortion between the probability distribution function (*pdf*) of SSM/I and that of rain gauge monthly rainfall values. The function parameters were evaluated using maximum likelihood estimation. The *pdf* distortion relationship was shown by Anagnostou et al. (1999) to lead to a power-law adjustment of the SSM/I monthly rainfall accumulations. Anagnostou et al (1999) has provided proof-of-concept of this approach on the basis of 10 years (1987-97) of SSM/I observations over the Northern South America region, which includes the Amazon basin. The study showed a 45% (0.1) reduction (increase) in the SSM/I-gauge monthly rainfall root-mean-square differences (correlation) as a result of this non-linear adjustment.

It is noted that SSM/I is not the sole PM sensor to base global precipitation climatology. However, it has the advantage to be the longest PM observational dataset, which can be used to provide a consistent (single sensor) long-term (18+ years) analysis of precipitation patterns (regional, seasonal and inter-annual), signals and trends. The algorithms and gauge-merging techniques used for SSM/I can readily apply to the other PM sensors such as AMSR and AMSU (it is already applied on TMI).

2. PRIOR RESEARCH

Prof. Anagnostou and his colleagues have done extensive work on precipitation remote sensing from microwave (active and passive) sensors on-board satellite platforms. Specifically, they have developed rainfall retrievals for both overland (Grecu and Anagnostou, 2001 and Dinku and Anagnostou, 2005a,b) and oceanic (Grecu and Anagnostou 2002, Grecu et al. 2004, and Grecu and Olson, 2005) surface. Summary of the work and its significance compared to other satellite retrievals is discussed next.

Our overland retrieval algorithms are statistical in nature with primary input being the brightness temperature depression at 37 and 85 GHz, which occurs due to scattering by ice and other frozen hydrometeors above the freezing level. The Dinku and Anagnostou (2005a) approach is an overland rain estimation algorithm developed for the TRMM Microwave Imager (TMI). It uses passive microwave observations from multiple TMI channels, and TRMM Precipitation Radar (PR) rainfall estimates as reference to calibrate the algorithm parameters. The algorithmic components include: (i) selection of the most appropriate TMI channel for rain rate estimation over a given geographic region and season; (ii) delineation of the raining areas and classification of rain into convective and stratiform (C/S) types on the basis of multiple TMI channel observations; and (iii) developing brightness temperature-rain rate relationships for each rain type. The rain estimates are at 0.1-deg nominal grid resolution. The significance of regional variation for the PR-based TMI algorithm calibration was investigated over four different geographic regions: Africa, Amazon basin, Southern US, and South Asia. It was found that the best single TMI channel for overland rain retrieval is the 37 GHz. Global calibration (i.e., constant parameters) was found to be sufficient for all examined continental regimes except the mountainous region of South Asia (where 85 GHz gave better correlations). Recent results (Dinku 2005) also showed that seasonal variation on algorithm parameters is not significant for the Tropical continental regions, indicating the possibility of using a single (optimal) parameter set applied for the whole year. Dinku and Anagnostou (2005a) assessed the performance of the PR-calibrated TMI algorithm with respect to the latest (Version 6) TRMM-2A12 surface rain estimates (McCollumn and Ferraro 2003) and were found to perform better than TRMM-2A12.

Dinku and Anagnostou (2005b) extended their TMI approach to develop a PR-calibrated SSM/I overland rainfall algorithm. The challenge of this study was that SSM/I and PR sensors fly onboard two different satellite platforms with varying field-of-view, geometry and overpass times. To overcome the problem we calibrated the SSM/I algorithm using TMI and PR data, by re-mapping TMI data to the SSM/I sensor resolution. This calibration approach is particularly attractive, as it does not rely on the availability of matched PR and SSM/I data. It can readily use TRMM-PR and TMI observations to derive SSM/I algorithm parameters for the various tropical/sub-tropical continental regimes and seasons. Dinku and Anagnostou (2005b) have shown using PR data as reference that in comparison with GPROF6 (McCollumn and Ferraro 2003) their algorithm may improve SSM/I rain estimation error statistics. The most significant indication for improvement was with respect to the systematic (about 60% bias reduction) and random (an increase of 0.4 in Efficiency) error. Fig. 1 shows sample images of instantaneous rain fields derived from PR, TMI (Dinku and Anagnostou 2005a algorithm) and SSM/I (Dinku and Anagnostou 2005b and GPROF6 algorithms). The PR rainfall field is at 5-km resolution, while the TMI and SSM/I fields are at 10-km and 25-km resolutions, respectively. We note that TMI estimates exhibit rain rate patterns similar to those of PR. Yet the effect of spatial averaging is apparent in the data. The effect is even more evident in the SSM/I rainfall fields. Our algorithm's rainfall patterns exhibit better similarity with the PR compared to GPROF6. For the given case, GPROF6 overestimated low rain rate areas, and underestimated higher rain rate areas. Another point to note is that the error structure of DA05 algorithm is less spatially correlated than GPROF6 (see Fig. 2). This is important as spatial dependence of error can introduce additional biases in aggregated rainfall fields at coarser resolutions.

Starting from the premise that the cloud resolving model simulations currently supporting the radiometer rain retrievals over oceans may be insufficient to capture the whole distribution of precipitation profiles and associated brightness temperatures, we have developed (Grecu and Olson, 2005) a database of precipitation profiles and associated brightness temperatures directly from TRMM observations. The combined PR/TMI algorithm developed by Grecu et al. (2004) was used to retrieve precipitation profiles directly from TRMM observations. The application of the combined algorithm to one month of TRMM observations yielded a database of more than one million retrieved profiles and coincident TMI brightness temperatures. The database was organized to facilitate the efficient application of a Bayesian algorithm to estimate precipitation profiles from radiometer-only observations. In essence, the database of precipitation profiles is searched to find profiles that are compatible with the TMI observations and ancillary data; the compatible profiles are then combined to form a solution profile. The approach to the radiometer-only algorithm is illustrated in Fig. 3.

The newly derived Bayesian retrieval algorithm was applied to a few months of TMI data and the estimates were compared to the combined PR/TMI of Grecu et al. (2004). The comparison showed that the new Bayesian estimates are more consistent than the TRMM TMI facility algorithm (GPROF) with the combined TMI/PR estimates. Although some regional biases exist, those are generally smaller than the systematic differences between the GPROF and PR/TMI combined estimates. An example of monthly rain estimates from the new radiometer algorithm supported by the PR/TMI database (henceforth the Bayesian TMI-only algorithm supported by the combined PR/TMI database will be called the PR/TMI-based TMI algorithm) is shown in Fig. 4. Presented on the left hand side of the figure are global maps of PR/TMI-based TMI $0.5^0 x 0.5^0$ monthly estimates of precipitation water content at three different altitudes, while on the right hand side are differences between the PR/TMI-based TMI and combined PR/TMI $0.5^0 x 0.5^0$ monthly estimates. It is apparent from Fig. 4 that the PR/TMI-based TMI algorithm performance is not uniform. In some regions, e.g. the central-eastern part of the ITCZ, the algorithm tends to overestimate while in other regions (e.g. tropical western Pacific) the algorithm generally underestimates precipitation. These biases are caused by differences between east and western Pacific rain systems (Berg et al. 2002) and are an indication that the physical parameters used in the estimation, i.e. the Sea Surface Temperature (SST) and a Cloud Top (CT) estimate from the TMI observations along with the brightness temperature principal components at the pixel level, are insufficient to detect subtle differences in the rain systems. Both the magnitudes of precipitation estimates and the differences between the two algorithms decrease with altitude. We intend to apply the radiometer algorithm supported by the combined PR/TMI retrievals to SSM/I data. Because the methodology to derive the database of precipitation profiles and associated brightness temperatures is based on physical models, the adaptation of the TMI-algorithm of Grecu and Olson (2005) is readily achievable.

3. METHODOLOGY

The goal of the work was to develop an improved global (land and ocean) precipitation climatology on the basis of 18+ years (since 1987) of TRMM-calibrated and gauge-adjusted Special Sensor Microwave/Imager (SSM/I) rainfall fields. To achieve our goal we addressed the following specific objectives:

1. Integrate our newly developed schemes of TRMM-based calibration for TMI overland and ocean retrieval in a single SSM/I global rain estimation algorithm;
2. Reprocess the SSM/I orbit data on the basis of the above algorithm to derive a multi-year (1987-present) rainfall dataset at 0.25-deg nominal grid resolution, and from those derive aggregate fields up to 2.5 degrees and monthly space-time scales;
3. Evaluate regional adjustment functions for the SSM/I rain accumulations to correct for MDC and satellite sampling effects;

A general protocol is established that identifies the fundamental phases involved in this study: (1) The acquisition, preparation and priming of the data; (2) Apply our algorithms to derive the best quality SSM/I precipitation fields for the period 1987-present; (3) Determine the MDC adjustment to the SSM/I monthly estimates based on TRMM data; (4) Evaluate non-linear adjustments to SSM/I data on the basis of regional/monthly rainfall comparisons with gauge measurements; (5) Assess the results and compare against existing SSM/I products on the basis of independent observations; (6) Determine trends in SSM/I precipitation and compare to those derived from GPCP datasets. These aspects are discussed next.

3.1 Dataset

To address our objectives we compiled a database consisting of the following observations:

- TRMM PR and TMI: Tropics/Sub-tropics coverage, 1998-present;
- SSM/I: global coverage, 1987-present;
- Gauges measurements over the globe (see Fig. 5 for station locations) for a period spanning from 1987 to present.

3.2 SSM/I Precipitation Retrievals

As discussed above two algorithms was used for rainfall estimation from SSM/I observations for overland and ocean retrievals. The algorithms and issues regarding integration and potential extensions are discussed in the following sub-sections:

3.2.1 The overland SSM/I retrieval

Since the early SSM/I retrievals of Spencer et al. (1989) and Olson (1989), a number of algorithms have been developed, few of which have been for overland rain estimation. The most popular SSM/I overland rain retrievals are those of NOAA/NESDIS (Grody 1991; Ferraro and Marks 1995; and Ferraro 1997) and the Goddard scattering algorithm (GSCAT) developed at NASA/GSFC by Adler et al. (1994). Conner and Petty (1995) described additional techniques and made validation comparisons with the NOAA/NESDIS and GSCAT algorithms. The most recent version of an operational SSM/I rainfall algorithm is the Goddard Profiling (GPROF) algorithm that was extended by McCollum and Ferraro (2003) for overland rainfall estimation. This algorithm is calibrated using TRMM-PR and used to produce the latest version (GPROF6—Version 6) of global SSM/I rain estimates at NASA and NOAA.

Dinku and Anagnostou (2005b) have presented a SSM/I overland rain retrieval that is a follow up to the DA05 (Dinku and Anagnostou 2005a) algorithm originally developed for TMI. The DA05 algorithm uses passive microwave (PM) observations from multiple channels, and TRMM Precipitation Radar (PR) rainfall estimates (rainfall rates and precipitation classification information) as reference to calibrate its parameters. The algorithm consists of the following components: (i) selection of the most appropriate PM channel over a given region; (ii) delineation of rain areas and classification of precipitation into Convective and Stratiform (C/S) type; and (iii) selection of the optimal brightness temperature-rain rate relationship for each rain type. The standard deviation of the 85-GHz brightness temperature array surrounding a PM pixel, and the 85-GHz Polarization Corrected Temperature (PCT—Spencer et al. 1989) of that pixel are used as predictors for discriminating rainy from non-rainy pixels. These predictors are regressed against binary PR-derived rain/no-rain classification estimates over land. The model for C/S classification is also a multi-linear regression type involving seven parameters extracted from the different PM channels. The reference data used for C/S classification algorithm calibration come from the PR (TRMM-2A23) rain type product. The probability matching technique is used to derive brightness temperature-rain rate (Tb-RR) relationships. As shown in Dinku and Anagnostou (2005a) stratiform precipitation cells' Tb-RR relationship is non-linear, while a linear relationship provides the best fit for the convective precipitation cells. A flowchart of the algorithm is shown in Fig. 6, while for details on the various algorithm components the reader is referred to Dinku and Anagnostou (2005a).

The major challenge in applying the PR-based calibration procedure of DA05 on SSM/I observations is the difficulty in matching (both in space and time) observations from the two sensors (PR and SSM/I). Dinku and Anagnostou (2005b) have explored two calibration scenarios that use sole TRMM data. The first approach maps the various TMI-channel brightness temperatures at the spatial resolutions of the corresponding SSM/I channels. The second (and simpler) TRMM-based calibration approach involves calibration of the DA05 retrieval algorithm on the basis of coincident PR rainfall and TMI brightness temperature data averaged at 0.25-deg grid resolution (instead of the original 0.1-deg used in DA05), without going through remapping. The rationale of both approaches is that the TMI and SSM/I channel frequencies are identical, with the only exception being the 21.3 GHz TMI channel that differs by ~1 GHz from the corresponding 22.23 GHz channel of SSM/I. The remapping procedure used in the first approach is a simple distance-weighted averaging, and it produces "SSM/I-like" brightness temperatures. After remapping, PR is used to calibrate the DA05 algorithm based on "SSM/I-like" TMI data at 0.25-deg grid resolution. Dinku and Anagnostou (2005b) have shown that remapping procedure produces reasonable "SSM/I-like" brightness temperatures. Dinku and Anagnostou (2005b) after comparing the performance achieved by each approach concluded that the second scenario performs the best. In addition, they concluded that best performance is achieved when the rain delineation and C/S classification parameters are evaluated at 0.25-deg while the Tb-RR relationship parameters are evaluated at 0.1-deg resolution. Their conclusion indicates that calibration of rain rate relationships at higher resolution gives better results even though the parameters are applied to lower resolution data, while this is not applicable in the evaluation of rain area and C/S classification parameters. This is because in the case of regression, the transition from 0.1 to 0.25-deg grids involves consistent averaging of both regression parameters (i.e., brightness temperature and rain rate), while this is not the case for rain area delineation and C/S classification. Consistently with the findings of Grecu and Anagnostou (2005b) the DA05 algorithm devised in this work uses rain delineation and C/S classification parameters computed at 0.25 deg, while the Tb-RR regression parameters were determined from PR-calibration of TMI at 0.1-deg resolution.

Dinku and Anagnostou (2005a) had investigated regional differences in the DA05 algorithm calibration. With the exception of the mountainous areas in South Asia it was noted that a global algorithm would perform similarly with a regionally calibrated algorithm. The 37 GHz was found to be the most suitable PM channel for Tb-RR rain relationships. It was noted, however, that for satellite pixels with mountainous background the 85 GHz might be more suitable than 37 GHz for rainfall rate relationships. This was indicated for the TMI retrieval over the mountainous complex in South Asia. More work on this aspect is needed to verify the results in other mountainous regions in Tropics and Sub-Tropics. Another aspect of the TRMM-based calibration is the extrapolation of the algorithm parameters over regions not covered by TRMM (mid latitudes). Chronis et al. (2004) has demonstrated through comparison with gauge data in central Europe that using the DA05 algorithm with parameters calibrated by TRMM over the continental US could result in good accuracy SSM/I retrievals over Europe (where TRMM data are not available). On the basis of collective evidence from our past studies (Dinku and Anagnostou 2005a,b and Chronis et al. 2004) we use the DA05 algorithm with global parameters calibrated using data from all the continental regimes under TRMM-PR coverage, with the exception of the mountainous regions where we conduct separate calibration (including selection of the best PM channel).

On-going work by Dinku and Anagnostou (2006) has also explored the significance of seasonal calibration of DA05 algorithm parameters. They investigated four continental regimes US, Africa, Amazon and South Asia. The conclusions from this study are that the effect of seasonal calibration versus using a global parameter set is negligible. However, they found differences in the accuracy of rain retrieval among the different seasons, such as: (1) the pre-monsoon season offers the best accuracy in all regions; (2) the worst accuracy for the Africa and Amazon regions is during the post-monsoon season, while over South Asia it is during the monsoon season. In the second year of this work we plan to further explore seasonal calibration significance before we decide on a single (or multi-season) set of algorithm parameters.

Our overall observation based on results presented in Dinku and Anagnostou (2005a,b) and on-going work by Dinku (2005) is that DA05 algorithm applied on SSM/I and TMI data offers improvements over GPROF6 used to derive the PM rainfall datasets in GPCP. For example, Dinku and Anagnostou (2005b) have shown that SSM/I rain estimation over Africa using DA05 algorithm exhibits 60% less bias and a 0.4 increase in the Efficiency score [defined as: $1 - Var(Error)/Var(PR\_rain)$] compared to GPROF6. This is also supported by the sample images of instantaneous rain fields derived from PR, TMI (DA05 algorithm) and SSM/I (DA05_SSM/I and GPROF6 algorithms) observations shown in Fig. 1. As discussed in a previous section, the SSM/I-DA05 rainfall patterns exhibit better similarity with the PR compared to the SSM/I-GPROF6. The overall statistical agreement between PR, SSM/I and TMI estimates is presented in Fig. 7 that shows the cumulative distribution functions (CDF) of the different algorithm estimates. As shown in the figure, the SSM/I-DA05 CDF is closer to the PR CDF compared to the SSM/I-GPROF6 CDF. An important point to note from both figures is that estimates from DA05 algorithm applied on TMI data (TMI-DA05 results) are associated with a 46% decrease (0.1 increase) in random error (correlation) relative to corresponding estimates from DA05 algorithm applied on SSM/I data (SSM/I-DA05). This indicates the great advantage gained by the increased resolution TMI observations, at the cost, though, of a smaller swath, which penalizes the use of the data in terms of sampling.

3.2.2 The oceanic SSM/I retrieval

The algorithm of Grecu et al (2005) was adapted and applied to estimate precipitation over oceans from SSM/I observations. As previously mentioned, the algorithm builds upon Prof. Anagnostou's previous work and provides a flexible, physical approach to incorporate into retrievals the information contained in the PR/TMI observations. The Bayesian estimation procedure on which the algorithm is based is similar in essence to other Bayesian procedures for estimating rain from radiometer observations (see for example Kummerow et al. 2001). That is, the estimation relies on a large database of precipitation profiles and associated brightness temperatures and a searching procedure is employed to determine the profiles in the database whose brightness temperatures are similar to the observed brightness temperatures. A statistical averaging is employed to provide a unique solution when more than one profile similar in terms of brightness temperatures to the observations exist.

The main difference between our approach and most of the previous approaches resides in the fact that the database is constructed directly from TRMM observations. In many instances, cloud resolving model (CRM) simulations are considered for constructing the databases or the parameterizations needed in passive microwave retrievals. They are physically based, flexible, and can shed light on phenomena difficult to understand and investigate from direct observations. However, there are serious drawbacks associated with the use of CRMs. First, the precipitation distribution in nature may be different from that simulated by CRMs. This is because CRMs are initialized using a relatively small set of large-scale environmental conditions that may not be statistically representative of the distribution of large-scale environments in nature. Second, CRMs might be deficient in handling ice processes, resulting in distributions of simulated 85-GHz brightness temperatures different from those observed in nature (Bauer, 2001). These drawbacks may be responsible for the differences between precipitation estimates from the version 5 TRMM Precipitation Radar (PR) and TRMM microwave imager (TMI) algorithms (Kummerow et al. 2001). Although these differences are reduced in the version 6 algorithms, some discrepancies still exist between the PR and TMI estimates (these will be illustrated in Section 3). From this perspective, but also for the benefit of future precipitation satellite missions, it is desirable to construct a precipitation-brightness temperature database free from the weaknesses of databases derived from current CRM simulations. Such a database can be constructed from a large set of precipitation profiles and associated brightness temperatures derived directly from TRMM observations. The combined algorithm of Grecu et al. (2004) is used in this respect. The combined algorithm derives solutions consistent with both the PR and TMI observations. This consistency is ensured through physical models that simulate the PR reflectivities and the TMI brightness temperatures and an objective mathematical is used to determine the precipitation profiles that yield the PR reflectivities and TMI brightness temperatures closest to the actual observations. Although in the retrieval process only the TMI brightness temperatures need to be simulated, once the final solution is determined brightness temperatures corresponding to different radiometers, e.g. SSM/I, can be readily simulated. Thus, a large database of precipitation profiles and associated SSM/I brightness temperatures can be readily constructed. Schematic demonstration of the process for constructing the database and further using it for passive microwave retrievals is presented in Fig. 3. As noted in the figure, PR and TMI observations are combined to retrieve precipitation profiles (vertical lines) in the overlap swath using the Grecu et al. (2004) approach. Brightness temperatures were then simulated using a physical model based on the combined PR/TMI observations for selected PM frequencies of the SSM/I sensor resolutions. These retrieved profiles form the precipitation-brightness temperature database for our SSM/I oceanic retrieval algorithm. Application of the database to SSM/I observations was done be through the classic Bayesian approach. Namely, SSM/I brightness temperatures were used to find radiatively compatible precipitation profiles in the database. The compatible profiles were then combined to form the solution profile.

A significant difference between our approach and other Bayesian radiometer retrieval algorithms is the organization of the database. The database is stratified by an estimate of the SST and passive-based estimate of the cloud top height, more precisely the PR echo top height (ET). The ET estimate is simply derived by regressing the simulated brightness temperatures in the database against the PR echo top height. The linear regression explains more the 75% of the total variation in the PR ET. Given the good performance in estimating the ET and the broad distribution of ET, the ET estimator is an effective parameter in determining the regions of the database where the solution is sought. This makes the solution computationally effective in spite of the large size of the database (approximately 20,000 profiles), which is significantly larger than the current GPROF's database.

As already mentioned, results show that our Bayesian estimates are more consistent than the TRMM TMI facility algorithm (GPROF) with the combined PR/TMI estimates. Given the use of PR observations, the PR/TMI estimates are considered more reliable rain estimates than any passive-only rain estimates, and therefore, considered as a reference. It is expected that our Bayesian algorithm supported by the TRMM database will produce superior rain estimates (and consistent with the TRMM PR/TMI) when applied to SSM/I observations. Furthermore, we have identified in our database a fairly large number of profiles with low freezing levels (lower than 2.0 km), which makes us believe that the algorithm will perform satisfactorily at mid and high/low latitudes as well. Finally, given that both the statistical overland and Bayesian ocean retrievals are formulated based on the same reference dataset (i.e., TRMM data) we expect consistent results over land and ocean.

3.2.3 Integration and open issues

As stated above the advantage of the two algorithms is that they are based on the same calibration dataset, i.e. PR and TMI over both land and ocean. A land/ocean/coast mask was devised to facilitate the selection of the appropriate algorithm. At coastal areas we initially used the statistical land retrieval algorithm, but these pixels were flagged uncertain. There are open issues associated with PM rainfall estimation that need further research. The two major ones are:

- Rain estimation over mountainous regions. Currently on-going research by Dinku (2005) shows that there are differences in the algorithm calibration for PM pixels located over mountainous terrain versus other areas. An important difference is that of the selection of the most appropriate PM channel to relate to rainfall. Dinku and Anagnostou (2005a) found that the 37 GHz is superior to the typically used 85 GHz over all major convective regions that are non-mountainous.

However, in regions associated with complex terrain the 85 GHz is the channel giving the best correlation with rainfall. We are currently investigating this issue for all mountainous areas located within the TMI coverage. Results from this research will be implemented in the newly developed SSM/I rainfall algorithm.

- The Convective/Stratiform classification. The DA05 performance to classify a satellite pixel as convective vs. stratiform is not high (Dinku and Anagnostou 2005a showed that we can explain about 30% of the total variance). In the same study we showed that by improving C/S classification (using the C/S classification from PR) alone we could get up to 35% reduction in the rain estimation error variance. Consequently, a definitive path to further reduce PM retrieval uncertainty is through the better classification of precipitation. This could be achieved by introducing information on the life cycle of the storm. A way to do that is using cloud-tracking information extracted from IR data and combining it with the PM channel classification parameters. This will be a subject of future research.

3.3 Deriving the SSM/I Precipitation Dataset

We developed an automated procedure that applies our combined ocean/land SSM/I retrieval on all SSM/I orbits since 1987 and retrieves surface rainfall rates, cloud top height (only for over ocean), and convective/stratiform precipitation index at 0.25-deg nominal grid resolution. Potentially, our procedure could be implemented at NASA as well as at NOAA/NESDIS for future processing (or re-processing) of SSM/I data. SSM/I products have been aggregated at different resolutions ranging from 0.5-deg/daily to 2.5 deg/monthly. The aggregated datasets at different resolutions include the following parameters: (1) average conditional rainfall rate (in mm/h), (2) mean, max and minimum cloud top height (in km), (3) rain fraction (in %), and (4) convective precipitation fraction (in %). Basic error statistics of the SSM/I monthly estimates were evaluated at various spatial resolutions through comparison with the ECMWF gauges and limited buoy data in the Pacific and Atlantic. For this purpose, over land we selected pixels with more than 4 gauges per pixel to evaluate statistics. We expect to make our validated SSM/I rainfall products and error statistics publicly available at the end of the second year of the project.

3.4 Evaluate Diurnal and Sampling Effects

The effects of mean diurnal cycle (MDC) of precipitation and satellite sampling were assessed on the basis of two approaches. The first approach uses the TMI rainfall products at sensor resolution to derive the MDC within the ±40-deg TMI latitudinal zone. The second approach uses the statistical algorithm of Anagnostou et al. (1999) to quantify non-linear adjustments to the gridded monthly SSM/I rainfall estimates on the basis of the ECMWF global gauge network measurements. The schemes are discussed next.

3.4.1 MDC correction

The globe was divided in a grid box of 5-deg resolution. The TMI rainfall estimates from each grid cell over the eight years of data were averaged at hourly intervals to derive the climatological mean precipitation at each hour. The MDC correction factor was then determined from the following formulae:

$$f(u;s) = \left(1 / \overline{R(u,s)}\right) \sum_{A_h(u)} R(u,h,s) \qquad (1)$$

where *R(u,h,s)* is the mean TMI rainfall of grid cell "u" at hour "h" and season "s". The $\overline{R(u,s)}$ represents the mean TMI rainfall at grid cell "u" of season "s". $A_h(u)$ represents the time domain (within the nearest hour) of SSM/I overpasses over grid cell "u". The significance of deriving MDC correction factors for different seasons was investigated before applying the MDC corrections to SSM/I data. If we find insignificant seasonal variations in MDC we will use single MDC correction factors representative of all seasons combined. Furthermore, we plan to examine the regional variations of MDC correction factor. On the basis of the above analysis we may change the grid box to coarser or finer cell resolution. The significance of MDC correction to SSM/I rainfall climatology will by assessed using the gauge network data (both ECMWF and other local data). It is noted that MDC correction may only apply on the Tropics/Sub-Tropics (±40-deg latitude) where we have available TMI data. At mid-latitudes we cannot apply any MDC correction, and we will rely solely on the non-linear adjustment to be derived from SSM/I-gauge comparisons. This is discussed next.

3.4.2 Non-linear rain gauge-based adjustment

The second scheme is the method of Anagnostou et al. (1999). The method utilizes a statistical concept, which evaluates the difference between two instruments (i.e., the SSM/I and the ECMWF global gauge network) in terms of their probability density functions (*pdf*). The two instruments are assumed to measure the same variable but with varying degrees of accuracy. The less reliable measurable (i.e., the SSM/I retrieval) is assumed to be a "distortion" of the other more definitive measurable (grid-average ECMWF rainfall measurement). The distortion is defined as:

$$g_1(x)= \exp[\alpha+\underline{\beta}h(x)]\, g(x) \qquad (2)$$

where $g(x)$ and $g_1(x)$ are the *pdf*s of the more (ECMWF) and less (SSM/I) reliable instruments, accordingly (Kay and Little, 1987). The exponential function is the *pdf* distortion factor, with $h(x)$ being a polynomial of x with parameter vector $\underline{\beta}$. Calculation of the *pdf* distortion factor parameters is done using maximum likelihood estimation (Fokianos et al., 1998). Derivations of the main equations used for parameter estimation are discussed in Anagnostou et al. (1999). Anagnostou et al. (1999) have shown that the distortion function can be used to evaluate a non-linear (i.e. power-law) adjustment relationship for the less accurate SSM/I rainfall estimates for specified spatial scales. In this study we evaluated non-linear adjustments to our SSM/I monthly rainfall estimates at 0.5-deg resolutions. Details of the procedure are discussed next.

Suppose that **x** is a random sample of ECMWF-measured monthly rainfall rates at a specified space-time scale, and **y** is a corresponding random sample of SSM/I-retrieved rainfall rates at the same scale, with n_0 and n_1 sample sizes, respectively. The distortion function (Eq. 2) between **x** and **y** *pdf*s is used to quantify a power-law adjustment relationship for the SSM/I rainfall estimates:

$$R_{SSM/I_{adj}} = aR_{SSM/I}{}^{b} \qquad (3)$$

where $R_{SSM/I_{adj}}$ and $R_{SSM/I}$ are adjusted and unadjusted SSM/I monthly rainfall estimates at the selected spatial resolution. The parameters (a,b) of the adjustment relationship are determined by minimizing the following objective function with respect to a and b:

$$f = \frac{1}{n_1}\sum_{i=1}^{n_1}\left[\left(g_1\left(ay_i^b\right) - g_0(y_i)^{-1} g_1(y_i)\right)\cdot y_i\right]^2 \qquad (4)$$

where g_1 are the jumps of the step *cdf* function at values y_i. The g_0 is the distortion function, here it will be a second order polynomial: $g_0(y_i)=\exp[\alpha+\beta_1 y_i+\beta_2 y_i^2]$, with parameter values $\hat{\alpha}$, $\hat{\beta}_1$, and $\hat{\beta}_2$ being the roots of a system of equations described in Anagnostou et al. (1999) (see equations 4-6).

Application of the method to SSM/I rainfall fields was as following. First we aggregated SSM/I and ECMWF data at 0.5-deg monthly accumulations. We selected all SSM/I pixels with corresponding gauge data over large periods (8+ years). Then we selected common areas to determine the adjustment function parameters (a,b). The areas were selected large enough to include several SSM/I pixels with corresponding gauge measurements to ensure statistical significance in determining *pdf*s. Initially, we considered those areas to be the 5-deg grid cells used in MDC correction. For each grid cell we used the Anagnostou et al. (1999) method to determine the adjustment function, which was applied uniformly to all SSM/I pixels within that cell.

There are two aspects about this approach that need further discussion. First, we are making an assumption of uniformity over large areas for the adjustment function parameters. Anagnostou et al. (1999) conducted an experiment to determine the spatial variability of the adjustment function parameters over similar size areas and concluded that parameter values are more sensitive to the satellite overpass time (e.g., F8, F11, F13 versus F10) than geographic location. Another observation is that parameter a, which controls the satellite estimation bias, experiences higher fluctuations than b. The above observation indicates that the diurnal pattern of rainfall, which is spatially variable (Negri et al., 1994), is a dominant error factor for the SSM/I monthly rainfall. Consequently, the MDC adjustment prior to the gauge-based non-linear adjustment would serve well the purpose of correcting SSM/I monthly estimates for sampling effects. In regions where MDC adjustment is not applied (mid to northern/southern latitudes) we expect higher uncertainty. However, at mid and northern latitudes we have denser gauge networks, consequently more data to better determine sampling effects.

References

Adler, R.F., G.J. Huffman, A. Chang, R. Ferraro, P.-P. Xie, J. Janowiak, B. Rudolf, U. Schneider, S. Curtis, D. Bolvin, A. Gruber, J. Susskind, P. Arkin and E. Nelkin, 2003: The Version-2 Global Precipitation Climatology Project (GPCP) Monthly Precipitation Analysis (1979–Present). *Journal of Hydrometeorology*: Vol. 4, No. 6, pp. 1147–1167.

Anagnostou, E.N., A.J. Negri, and R.F. Adler, 1999: Statistical Adjustment of Satellite Microwave Monthly Rainfall Estimates over Amazonia. *Journal of Applied Meteorology*, Vol 38, 1590-98.

Bell, T.L., A. Abdullah, R.L. Martin, and G.R. North, 1990: Sampling errors for satellite-derived tropical rainfall: Monte Carlo study using a space-time stochastic model. *J. Geophys. Res*., 95, 2195-2206.

Berg, W., C. Kummerow and C. A. Morales. 2002: Differences between East and West Pacific Rainfall Systems. *J. Climate*, **15**, 3659–3672.

Chronis, T., E.N. Anagnostou, and T. Dinku, 2004: High-frequency Estimation of Thunderstorms via Satellite Infrared and a Long-Range Lightning Network in Europe, Quarterly Journal of the Royal Meteorological Society, Vol. 130 Part B No. 599, 1555-1575.

Conner, M. D., and G. R. Petty, 1998: Validation and intercomparison of SSM/I rain-rates retrieval methods over the continental Unites States. J. Appl. Meteor.,37, 679-700.

Dinku T. and E.N. Anagnostou, 2005: Investigating Seasonal PR-TMI Calibration differences, *Journal of Applied Meteorology* (submitted).

Dinku T., 2005: “Use of TRMM Precipitation Radar for Calibrating Overland Passive Microwave Rain Retrieval.” Ph.D. Thesis, Civil and Environmental Engineering Department, University of Connecticut, Storrs, CT.

Dinku T., and E.N. Anagnostou, 2005a: Regional Differences in Overland Rainfall Estimation from PR-Calibrated TMI Algorithm. *Journal of Applied Meteorology*: Vol. 44, No. 2, pp. 189–205.

Dinku T., and E.N. Anagnostou, 2005b: TRMM Calibration of SSM/I Algorithm for Overland Rainfall Estimation. Submitted to *Journal of Applied Meteorology* (in press).

Ferraro, R. R., and G. F. Marks, 1995: The Development of SSM/I rain-rate retrieval algorithms using ground-based radar measurements. J. Atmos. Oceanic Technol., 12,755-770.

Ferraro, R. R., 1997: Special sensor microwave imager derived global rainfall estimates for climatological applications. J. Geoephys. Res.,102, 16715-16735.

Fokianos, K., B. Kedem, J. Qin, J.L. Haferman, and D.A. Short, 1998: On Combining Instruments. J. Appl. Meteor. 37, 220-226.

Goody, R., J. Anderson, T. Karl, R. Bastald Miller, G. North, J. Simpson, G. Stephens, and W. Washington, 2002: Why monitor the climate? *Bull. Amer. Meteor. Soc.*, 83, 873-878.

Grecu, M, and W.S. Olson, 2005: Bayesian Estimation of Precipitation from Satellite Passive Microwave Observations Using Combined Radar-Radiometer Retrievals. Submitted to *J. Appl. Meteorol*.

Grecu, M., W.S. Olson and E.N. Anagnostou, 2004: Retrieval of Precipitation Profiles from Multiresolution, Multifrequency Active and Passive Microwave Observations. *Journal of Applied Meteorology*: Vol. 43, No. 4, pp. 562–575.

Grody, N.C., 1991: Classification of snow cover and precipitation using the Special Sensor Microwave Imager. J. Geoephys. Res., 96, 7423-7435.

Haddad, Ziad S., Im, Eastwood, Durden, Stephen L., Hensley, Scott. 1996: Stochastic Filtering of Rain Profiles Using Radar, Surface-Referenced Radar, or Combined Radar–Radiometer Measurements. *Journal of Applied Meteorology*: Vol. 35, No. 2, pp. 229–242.

Iguchi, T., T. Kozu, R. Meneghini, J. Awaka and K. Okamoto, 2000: Rain-profiling algorithm for TRMM precipitation radar. *J. Appl. Meteor*, 39, 2038-2052.

Kay, R., and S. Little, 1987: Transformations of the explanatory variables in the logistic regression model for binary data. Biometrika, 74, 495-501.

Kummerow, C., Y. Hong, W. S. Olson, S. Yang, S., R. F. Adler, J. McCollum, R. Ferraro, G. Petty, D.-B. Shin, and T. T. Wilheit, 2001: The Evolution of the Goddard Profiling Algorithm (GPROF) for rainfall estimation from passive microwave sensors. *J. Appl. Meteor*., 40, 1801–1820.

Kummerow, C., 1998: Beamfilling errors in passive microwave rainfall retrievals. *J. Applied Meteor.*, 37, 356-70.

McCollum, J.R. and R. Ferraro, 2003: Next generation of NOAA/NESDIS TMI, SSM/I, and AMSR-E microwave land rainfall algorithms. *J. Geophys. Res.-Atm*., 108.

Negri, A.J., E.N. Anagnostou, and R.F. Adler, 2000: A 10-Yr Climatology of Amazonian Rainfall Derived from Passive Microwave Satellite Observations. *Journal of Applied Meteorology*, Vol. 39, 42-56.

Negri, A.J., R.F. Adler, E.J. Nelkin, and G.J. Huffman, 1994: Regional rainfall climatologies derived from Special Sensor Microwave Imager (SSM/I) data. *Bull. Of Amer. Meteor. Soc*., 75(7), 1165-82.

Potter, G. L., and R. D. Cess, 2004: Testing the impact of clouds on the radiation budgets of 19 atmospheric general circulation models. *J. Geophys. Res*., 109, D02106, doi:10.1029/2003JD004018.

Smith, Eric A., Turk, F. Joseph, Farrar, Michael R., Mugnai, Alberto, Xiang, Xuwu. 1997: Estimating 13.8-GHz Path-Integrated Attenuation from 10.7-GHz Brightness Temperatures for the TRMM Combined PR–TMI Precipitation Algorithm. Journal of Applied Meteorology: Vol. 36, No. 4, pp. 365–388.

Spencer, R.W., H.M. Goodman, R.E. Hood, 1989: Precipitation Retrieval over Land and Ocean with the SSM/I: Identification and Characteristics of the Scattering Signal. J. Atmos. Oceanic Technol., 6,254-273.

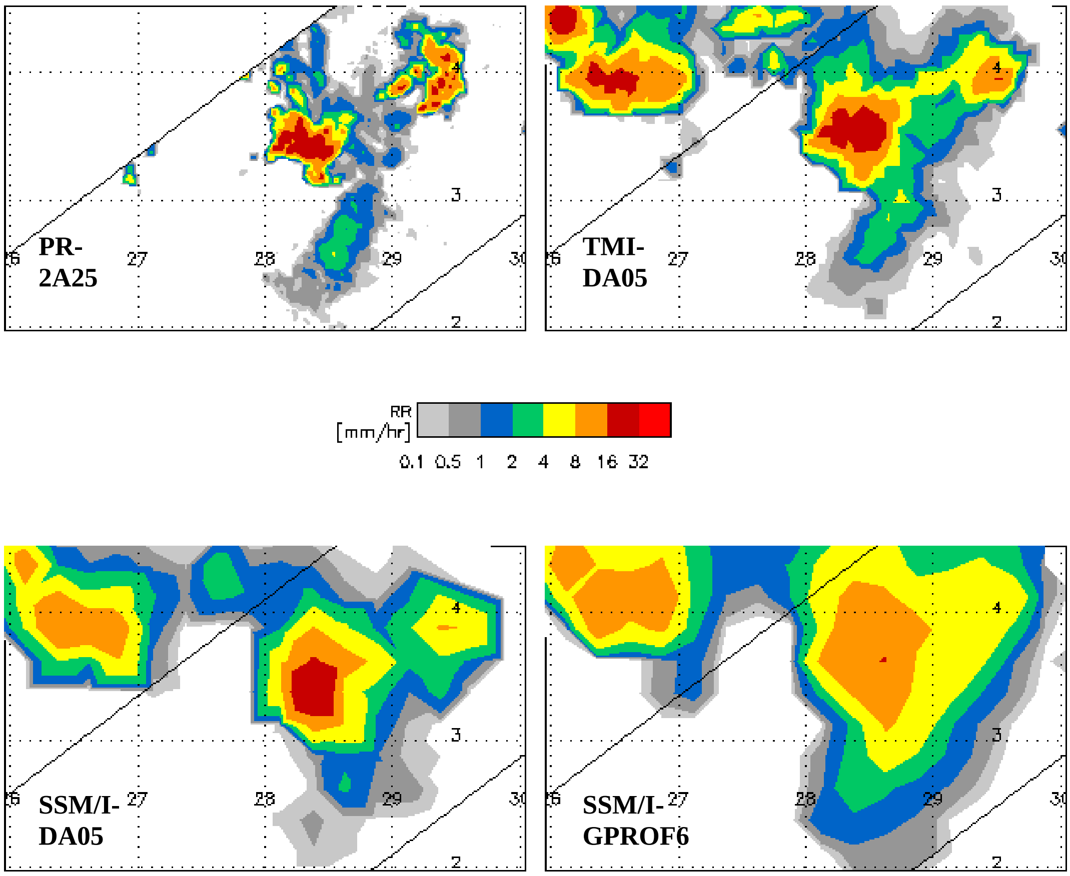

Figure 1: Examples of instantaneous rain rate maps retrieved from PR, TMI (Dinku and Anagnostou 2005a algorithm) and SSM/I (ALG2b—Dinku and Anagnostou 2005b, and GPROF6 algorithms). Lines show the PR swath.

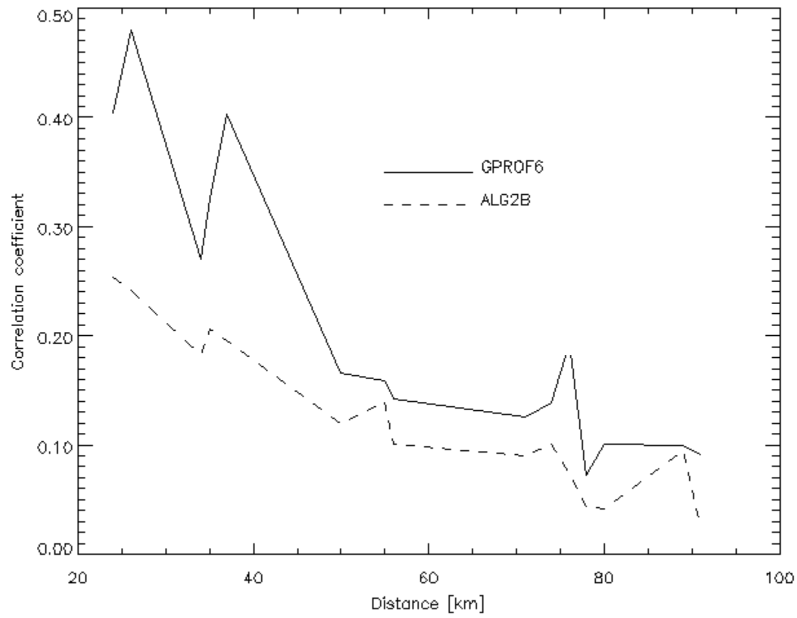

Figure 2: Spatial error correlations of SSM/I rain estimates retrieved from DA05 (dashed line) and GPROF6 (solid line) algorithms. Error is defined as the difference of SSM/I estimates versus PR rainfall rates.

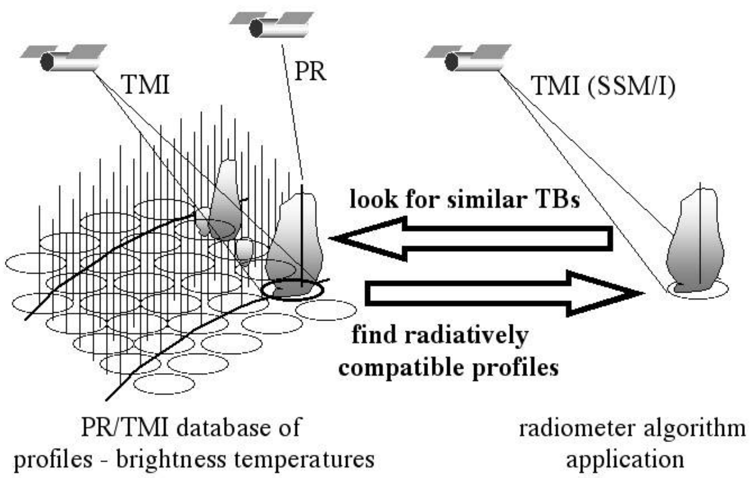

Figure 3: Schematic of the radiometer-only precipitation profile estimation method. On the left-hand side, PR and TMI observations are combined to retrieve precipitation profiles (vertical lines) in the overlap swath. These retrieved profiles form the precipitation-brightness temperature database for the radiometer-only algorithm. On the right-hand side, radiometer brightness temperatures (TB's) are used to find radiatively compatible precipitation profiles in the PR/TMI database. The brightness temperatures are derived using a physical model based on the combined PR/TMI observations for selected PM frequencies and sensor resolutions. The compatible profiles are combined to form the solution profile.

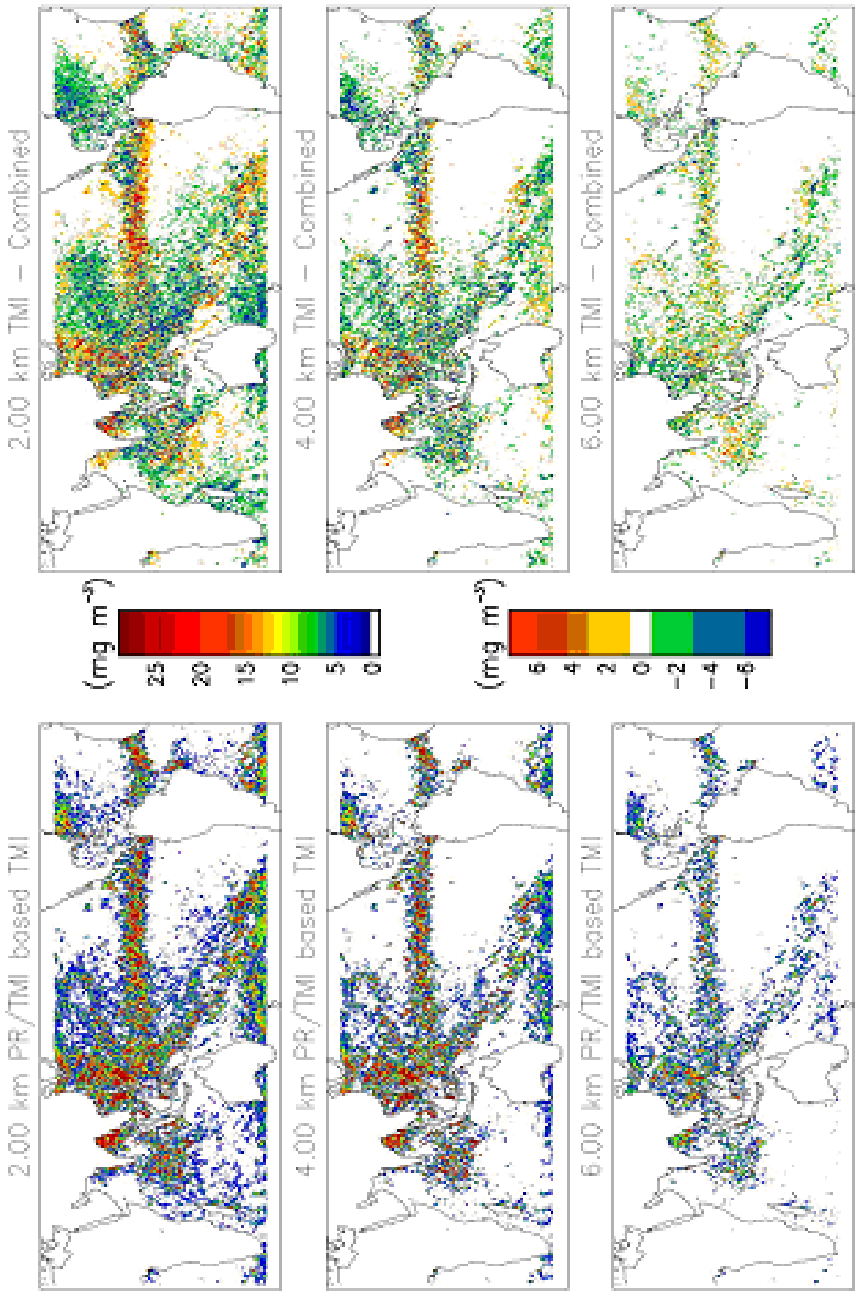

Figure 4: Monthly 0.5^0x0.5^0 estimates of precipitation water contents from the PR/TMI-based TMI algorithm at three different altitudes. The bottom panels show the actual estimates (i.e., PR/TMI-based TMI estimates), while the top panels show the differences between the PR/TMI-based TMI and the combined PR/TMI estimates.

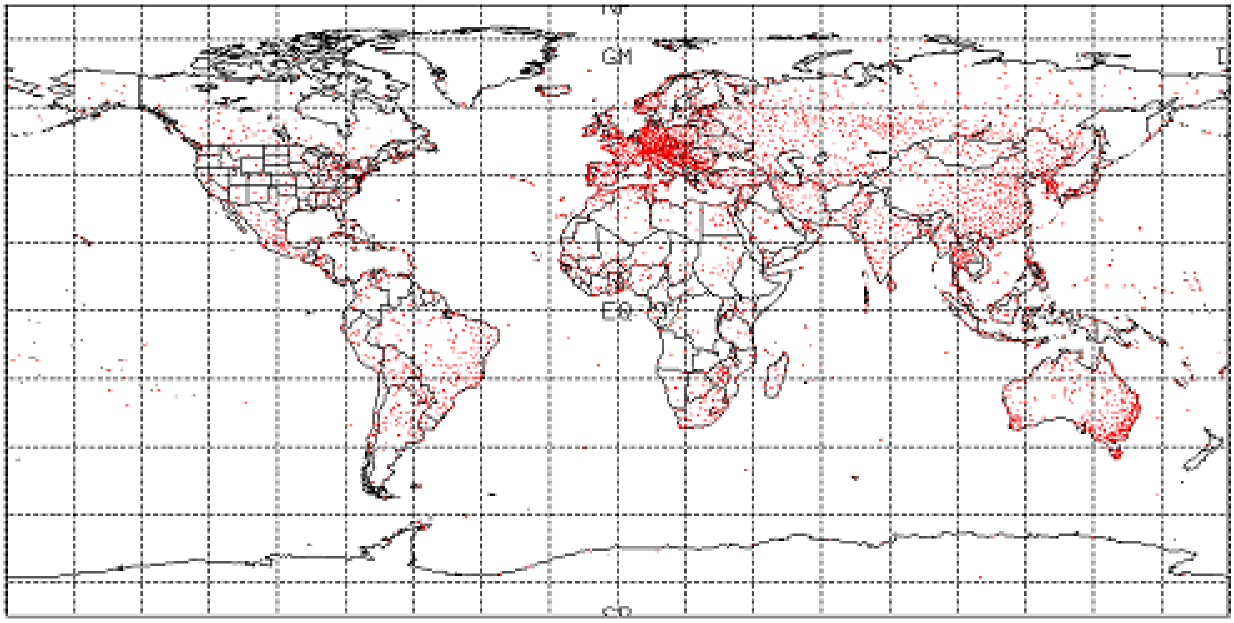

Figure 5: The ECMWF global gauge network.

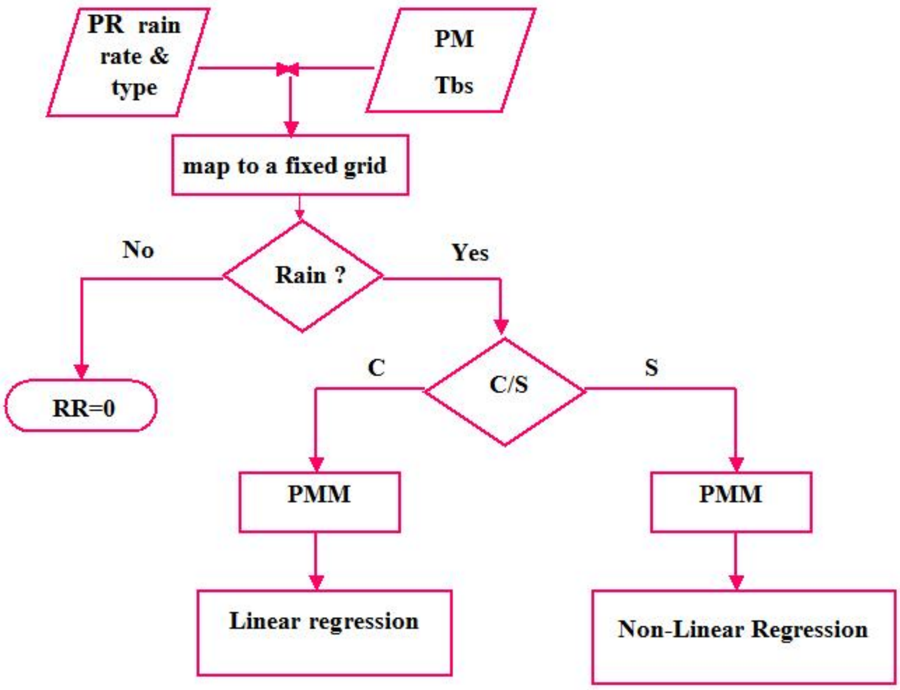

Figure 6: Flowchart of the DA05 overland passive microwave rainfall estimation algorithm

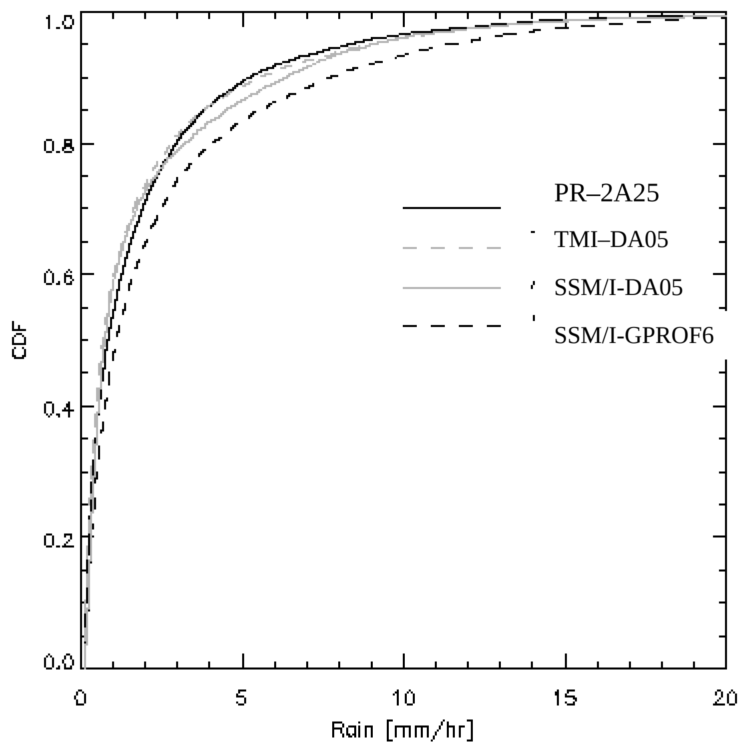

Figure 7: Cumulative Density Functions (CDF) of coincident overland rainfall rates (over Africa) retrieved by PR (2A-25 algorithm), TMI (DA05 algorithm), and SSM/I (DA05 & GPROF6 algorithms) sensor observations